Dynamic Analysis of a Motion Transformer Mimicking a Hula Hoop

C. X. Lu

C. C. Wang

C. K. Sung[1]
Professor
e-mail: cksung@pme.nthu.edu.tw

Department of Power Mechanical Engineering,
National Tsing Hua University,
Eng. 1, No. 101, Section 2,
Kuang-Fu Road,
Hsinchu, Taiwan 30013, R.O.C.

Paul C.P. Chao
Department of Electrical Engineering,
Institute of Imaging and Biophotonics,
National Chiao Tung University,
Hsinchu 30013, Taiwan

Hula-hoop motion refers to the spinning of a ring around a human body; it is made possible by the interactive force between the moving ring and the body. Inspired by the generic concept of hula-hoop motion, this study proposes a novel motion transformer design that consists of a main mass sprung in one translational direction and a free-moving mass attached at one end of a rod, the other end of which is hinged onto the center of the main mass. It is expected that the transformer is capable of transforming linear reciprocating motion into rotational motion. In addition, the transformer could be integrated with coils, magnets, and electric circuits to form a portable energy scavenging device. A thorough dynamic analysis of the proposed transformer system is conducted in this study in order to characterize the relationships between the varied system parameters and the chance of hula-hoop motion occurrence. The governing equations are first derived with Lagrange's method, which is followed by the search for steady-state solutions and the corresponding stability analysis via the homotopy perturbation method and the Floquet theory. Direct numerical simulation is simultaneously performed to verify the correctness of the approximate analysis. In this manner, the feasibility of the proposed design and the occurrence criteria of hula-hoop motion are assessed. [DOI: 10.1115/1.4001839]

1 Introduction

Inspired by the generic concept of hula-hoop motion, which occurs due to the interactive forces between the moving ring and the human body, this study proposes a novel motion transformer design that is capable of transforming linear vibro-motions into rotary motions. The proposed transformer consists of a main mass sprung in one translational direction and a free-moving mass attached at one end of a rod, the other end of which is hinged onto the main mass. Yoshitake et al. [1] developed a similar device consisting of a hula hoop and a generator for quenching the vibration of a structure or a machine while generating electric energy. By composing the resonance curve of rotating and nonrotating hula hoops, the operating curve revealed the performance of hula-hoop motion. Hatwal et al. [2] presented a dynamic analysis of a system with a very similar dynamic structure, but the analysis concentrated on the small-amplitude oscillatory motions of the free mass. In contrast, the free mass is expected to exhibit spinning motion, that is, rotational hula-hoop motion in this study when the rotational and oscillation frequency match. Additionally, Garira and Bishop [3] investigated the properties of different steady-state rotational solutions of a parametrically excited pendulum. Lenci et al. [4] presented rotational solutions and its stability of parametric pendulum via the perturbation method. Wu [5] proposed a rotational pendulum vibration absorber with a spinning support for decreasing vibrations. Furthermore, the phenomena of rotating behavior of the model with an unbalanced rotor were also investigated by researchers via the method of averaging [6–10], the Tikhonov method [11], and the multiple-scale perturbation technique [12].

The equations governing the motions of the main and free masses are first formulated based on the physical model. Because the equations are nonlinear, the search for steady-state solutions and the corresponding stability conditions is conducted in sequence. Since, in this study, the free mass is anticipated to revolve in the hula-hoop motion rather than the small-amplitude oscillatory motion, we adopt the homotopy perturbation method to solve the nonlinear dynamic equations for obtaining better approximate solutions [13–15]. After the approximate solutions are attained, the corresponding stability conditions are evaluated using the Floquet theory. On the basis of the obtained results, the design guidelines for determining transformer parameters to ensure the occurrence of hula-hoop motion are determined.

2 Physical Model and Governing Equation

Mimicking the hula-hoop motion, this study proposes a novel motion transformer design, as shown in Fig. 1(*a*), which consists of a main mass sprung in the *y*-direction and a free-moving mass attached at one end of a rod, the other end of which is hinged onto the center of the main mass.

In Fig. 1(*a*), M, m, k, c, c_m, R_m, and F denote the main mass, free mass, coefficient of the spring, damping capacity of the damper, rotational damping due to the friction between the pin and the hole, rotational radius between the center of the free mass and the pin, and the excitation force applied in the *y*-direction, respectively. The main mass is confined to move only in the *y*-direction. The free mass is assumed to be a point mass in Fig. 1(*a*) or a semicircle thin plate in Fig. 1(*b*). The main and free masses move parallel to the ground; no gravitational force acts on them. On the basis of the dynamic characteristics of the model, the motion of free mass is defined as $x_f = R_m \cos\theta$ and $y_f = y + R_m \sin\theta$. x_f and y_f denote the absolute displacements of the free mass in the *x*- and *y*-directions, respectively; y denotes the reciprocating motion of the main mass, and θ denotes the rotational angle of the free mass. By differentiating x_f and y_f with respect to time, the velocity of free mass in the *x*- and *y*-directions can be obtained as $\dot{x}_f = -R_m\dot{\theta}\sin\theta$ and $\dot{y}_f = \dot{y} + R_m\dot{\theta}\cos\theta$.

Then, the kinetic energy, T, and potential energy, V, caused by the deformation of the spring are expressed as

$$T = \frac{1}{2}M\dot{y}^2 + \frac{1}{2}m(\dot{x}_f^2 + \dot{y}_f^2) + \frac{1}{2}I\dot{\theta}^2 = \frac{1}{2}M\dot{y}^2 + \frac{1}{2}m(\dot{y}^2 + 2R_m\dot{y}\dot{\theta}\cos\theta + R_m^2\dot{\theta}^2) + \frac{1}{2}I\dot{\theta}^2 \quad (1)$$

$$V = \frac{1}{2}ky^2 \quad (2)$$

where I is the mass moment of inertia of the semicircle free mass. With the kinetic energy, potential energy, and generalized forces, the equations describing the motion of the system can be derived by using Lagrange's equations:

[1]Corresponding author.

Contributed by the Technical Committee on Vibration and Sound of ASME for publication in the JOURNAL OF VIBRATION AND ACOUSTICS. Manuscript received March 13, 2009; final manuscript received April 29, 2010; published online January 5, 2011. Assoc. Editor: Steven W Shaw.

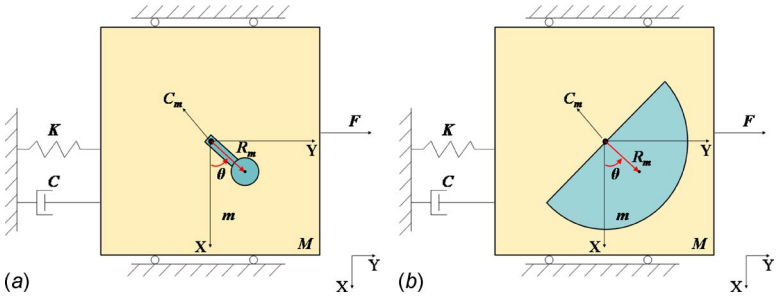

Fig. 1 Physical model of hula-hoop motion with (*a*) a point mass and (*b*) a semicircular thin plate as the free masses

$$\frac{d}{dt}\left(\frac{\partial T}{\partial \dot{y}}\right) - \frac{\partial T}{\partial y} + \frac{\partial V}{\partial y} = \Theta \tag{3}$$

$$\frac{d}{dt}\left(\frac{\partial T}{\partial \dot{\theta}}\right) - \frac{\partial T}{\partial \theta} + \frac{\partial V}{\partial \theta} = U \tag{4}$$

where $\Theta = F\cos(\omega t) - c\dot{y}$ and $U = -c_m\dot{\theta}$ are the generalized nonconservative forces. Thus, the equations governing the motion of the main mass and free mass are written as

$$(M+m)\ddot{y} + mR_m(\ddot{\theta}\cos\theta - \dot{\theta}^2\sin\theta) + c\dot{y} + ky = F\cos(\omega t) \tag{5}$$

and

$$(mR_m^2 + I)\ddot{\theta} + c_m\dot{\theta} = -mR_m\ddot{y}\cos\theta \tag{6}$$

where I is the mass moment of inertia of the semicircular thin plate. Equations (5) and (6) are expressed in nondimensional forms for conveniently analyzing the dynamic behaviors of the system:

$$q''(\tau) + 2\rho q'(\tau) + q(\tau) + \varepsilon[\theta''(\tau)\cos\theta(\tau) - (\theta'(\tau))^2\sin\theta(\tau)] = F_{\text{eq}}(\tau) \tag{7}$$

and

$$(1 + I_{\text{eq}})\theta''(\tau) + \xi_m\theta' + q''(\tau)\cos\theta(\tau) = 0 \tag{8}$$

where

$$\tau = \omega_n t, \quad \omega_n = \sqrt{\frac{k}{M+m}}, \quad q(\tau) = y(t)/R_m,$$

$$q'(\tau) = \dot{y}(t)/R_m\omega_n, \quad \theta(\tau) = \theta(t), \quad \theta'(\tau) = \dot{\theta}(t)/\omega_n,$$

$$\varepsilon = \frac{m}{M+m}, \quad F_{\text{eq}}(\tau) = \frac{F\cos(\alpha\tau)}{(M+m)R_m\omega_n^2}, \quad \alpha = \omega/\omega_n,$$

$$\rho = \frac{c}{2(M+m)\omega_n}, \quad \mathrm{s}_m = \frac{c_m}{mR_m^2\omega_n}, \quad I_{\text{eq}} = \frac{9\pi^2}{32} - 1$$

The prime denotes the derivative with respect to the nondimensional time τ. ω_n and ω are the natural frequency of the system and the excitation frequency, respectively. In addition, α is the nondimensional frequency of excitation.

3 Approximate Solutions

3.1 Homotopy Perturbation Method. The homotopy perturbation method proposed by He [14] possesses the advantages of the traditional perturbation methods and those of the homotopy technique, which will be described briefly. One can employ this method to solve nonlinear differential equations. A general nonlinear equation can be in the form of

$$A(V) - f(\tau) = 0 \tag{9}$$

where A is a general differential operator with the linear part, L, and the nonlinear part, N, and $f(\tau)$ is a known analytic function. A homotopy $V(\tau,p):\Omega\times[0,1]\rightarrow\Re$ can be constructed with this method to satisfy

$$H(V,p) = (1-p)[L(V) - L(U_0)] + p[A(V) - f(\tau)] = 0 \tag{10}$$

or

$$H(V,p) = L(V) - L(U_0) + pL(U_0) + p[N(V) - f(\tau)] = 0 \tag{11}$$

where $p\in[0,1]$ is an embedding parameter and $\tau\in\Re$. U_0 is an initial approximation of Eq. (11). When the embedded parameter p is zero, the equation is of the linear system; as p is unit, it recovers to the original one, which are shown as follows:

$$H(V,0) = L(V) - L(U_0) = 0 \tag{12}$$

$$H(V,1) = A(V) - f(\tau) = 0 \tag{13}$$

Herein, the process is termed deformation in topology, and Eqs. (12) and (13) are homotopic. After the homotopy deformation, Eq. (10) or Eq. (11) is termed the perturbation equation with an embedding parameter p considered as a small parameter.

3.2 Solution Procedures. This study employs the homotopy perturbation method [15] to solve the nonlinear differential Eqs. (7) and (8). We first establish these two equations as the homotopy $V_q(\tau,p):\Omega\times[0,1]\rightarrow\Re$, which satisfies

$$L(V_q) - L(U_{0q}) + pL(U_{0q}) + pN(V_\theta) - pf(\tau) = 0 \tag{14}$$

$$L(V_\theta) - L(U_{0\theta}) + pN(V_{\theta q}) + pL(U_{0\theta}) = 0 \tag{15}$$

When the hula-hoop motion occurs, i.e., the free mass continuously spins around the center of the main mass, the initial approximations of Eqs. (7) and (8) can be assumed in the following forms with four unknowns q_1, u_1, β, and γ:

$$U_{0q} = q_1\cos(f_q\tau - \beta) \tag{16}$$

$$U_{0\theta} = \alpha\tau + u_1\cos(f_u\tau - \gamma) \tag{17}$$

where $f_q = \alpha$ and $f_u = 2\alpha$.

Since p is an embedded parameter through the homotopy technique from Eq. (11), one can assume that the approximate solution of Eqs. (14) and (15) have the form

$$V_q = V_{0q} + pV_{1q} + p^2V_{2q} + \cdots \tag{18}$$

$$V_\theta = V_{0\theta} + pV_{1\theta} + p^2V_{2\theta} + \cdots \tag{19}$$

Then, substituting Eqs. (18) and (19) into Eq. (14) yields the approximate solution of Eq. (14),

$$L(V_{0q}) - L(U_{0q}) + p[L(V_{1q}) + L(U_{0q}) + N(V_{0\theta}) - f(\tau)] + p^2[L(V_{2q}) + N(V_{1\theta})] + \cdots = 0 \tag{20}$$

Equating the terms with identical powers of p, the following relations can be derived:

$$L(V_{0q}) - L(U_{0q}) = 0 \tag{21}$$

$$L(V_{1q}) + N(V_{0\theta}) + L(U_{0q}) - f(\tau) = 0 \tag{22}$$

From Eq. (21), one has

$$V_{0q} = U_{0q} = q_1 \cos(f_q\tau - \beta) \tag{23}$$

From Eq. (22), the nonlinear terms, $N(V_{0\theta})$, include $\varepsilon(\theta')^2 \sin\theta$ and $\varepsilon\theta''\cos\theta$ of Eq. (7), in which ε is the mass ratio of the system, and others belong to linear terms except that the excitation F is an analytic function, $f(\tau)$. Then, substituting the initial approximation Eq. (17) into the nonlinear terms yields

$$\begin{aligned}\varepsilon(\theta')^2\sin\theta &= \varepsilon[\alpha - u_1 f_u \sin(f_u\tau - \gamma)]^2 \sin[\alpha\tau + u_1\cos(f_u\tau - \gamma)] \\ &= \varepsilon\{\alpha^2 - 2\alpha u_1 f_u \sin(f_u\tau - \gamma) + [u_1 f_u \sin(f_u\tau - \gamma)]^2\} \\ &\quad \times\{\sin\alpha\tau\cos[u_1\cos(f_u\tau - \gamma)] \\ &\quad + \cos\alpha\tau\sin[u_1\cos(f_u\tau - \gamma)]\} = \varepsilon\{\{\alpha^2 \\ &\quad - 2\alpha u_1 f_u \sin(f_u\tau - \gamma) + [u_1 f_u \sin(f_u\tau \\ &\quad - \gamma)]^2\}\sin\alpha\tau\cos[u_1\cos(f_u\tau - \gamma)] + \{\alpha^2 \\ &\quad - 2\alpha u_1 f_u \sin(f_u\tau - \gamma) + [u_1 f_u \sin(f_u\tau \\ &\quad - \gamma)]^2\}\cos\alpha\tau\sin[u_1\cos(f_u\tau - \gamma)]\}\end{aligned} \tag{24}$$

With Neumann's expansion [16], the equation becomes

$$\begin{aligned}\varepsilon(\theta')^2\sin\theta &= \varepsilon\{\{\alpha^2 - 2u_1 f_u \sin(f_u\tau - \gamma) + [u_1 f_u \sin(f_u\tau \\ &\quad - \gamma)]^2\}\sin\alpha\tau[J_0 - 2J_2\cos 2(f_u\tau - \gamma) + 2J_4\cos 4(f_u\tau \\ &\quad - \gamma) - \cdots] + \{\alpha^2 - 2u_1 f_u \sin(f_u\tau - \gamma) + [u_1 f_u \sin(f_u\tau \\ &\quad - \gamma)]^2\}\cos\alpha\tau[2J_1\cos(f_u\tau - \gamma) - 2J_3\cos 3(f_u\tau - \gamma) \\ &\quad + 2J_5\cos 5(f_u\tau - \gamma) - \cdots]\}\end{aligned} \tag{25}$$

where J's represent the Bessel's coefficients as

$$J_n(u_1) = \left(\frac{u_1}{2}\right)^n \sum_{k=0}^{\infty} \frac{\left(-\frac{u_1^2}{4}\right)^k}{k!(n+k)!}, \quad n = 0,1,2,3,4,5,\ldots \tag{26}$$

The Bessel function is simplified as

$$J_n(u_1) \cong \frac{u_1^n}{2^n n!} \tag{27}$$

where $k=0$ with the consideration of $|u_1| < 0.5$.

The equation can be expanded with trigonometric function, but for simplicity, the harmonic function with the lowest frequency α is kept in the derivation; furthermore, there are no harmonic functions with frequency 2α in the expansion. After the above, we can equate the nonlinear term $\varepsilon(\theta')^2\sin\theta$ with $\sin\alpha\tau$ and $\cos\alpha\tau$ as follows:

$$\begin{aligned}\varepsilon(\theta')^2\sin\theta &= \varepsilon\sin(\alpha\tau)\left[\left(\alpha^2 + \frac{u_1^2 f_u^2}{2}\right)J_0 + \left(\alpha^2 + \frac{u_1^2 f_u^2}{2}\right)J_1\sin\gamma \right. \\ &\quad + (-2\alpha u_1 f_u)\frac{J_0 + J_2}{2}\sin\gamma - \left(-\frac{u_1^2 f_u^2}{2}\right)J_2 \\ &\quad \left. + \left(-\frac{u_1^2 f_u^2}{2}\right)\frac{J_1 - J_3}{2}\sin\gamma\right] + \varepsilon\cos(\alpha\tau)\left[\left(\alpha^2\right.\right. \\ &\quad \left.\left. + \frac{u_1^2 f_u^2}{2}\right)J_1\cos\gamma + (-2\alpha u_1 f_u)\frac{J_0 + J_2}{2}\cos\gamma\right. \\ &\quad \left. + \left(-\frac{u_1^2 f_u^2}{2}\right)\frac{J_1 - J_3}{2}\cos\gamma\right]\end{aligned} \tag{28}$$

According to Eq. (24)'s derivation, the nonlinear term $\varepsilon\theta''\cos\theta$ can be as follows:

$$\begin{aligned}\varepsilon\theta''\cos\theta &= \varepsilon[-u_1 f_u^2\cos(f_u\tau - \gamma)]\cos[\alpha\tau + u_1\cos(f_u\tau - \gamma)] \\ &= \varepsilon[-u_1 f_u^2\cos(f_u\tau - \gamma)]\{\cos\alpha\tau\cos[u_1\cos(f_u\tau - \gamma)] \\ &\quad - \sin\alpha\tau\sin[u_1\cos(f_u\tau - \gamma)]\} = \varepsilon\{[-u_1 f_u^2\cos(f_u\tau \\ &\quad - \gamma)]\cos\alpha\tau\cos[u_1\cos(f_u\tau - \gamma)] - [-u_1 f_u^2\cos(f_u\tau \\ &\quad - \gamma)]\sin\alpha\tau\sin[u_1\cos(f_u\tau - \gamma)]\}\end{aligned} \tag{29}$$

With Neumann's expansion [16], the equation becomes

$$\begin{aligned}\varepsilon\theta''\cos\theta &= \varepsilon\{[-u_1 f_u^2\cos(f_u\tau - \gamma)]\cos\alpha\tau\cos[u_1\cos(f_u\tau - \gamma)] \\ &\quad - [-u_1 f_u^2\cos(f_u\tau - \gamma)]\sin\alpha\tau\sin[u_1\cos(f_u\tau - \gamma)]\} \\ &= \varepsilon\{[-u_1 f_u^2\cos(f_u\tau - \gamma)]\cos\alpha\tau[J_0 - 2J_2\cos 2(f_u\tau - \gamma) \\ &\quad + 2J_4\cos 4(f_u\tau - \gamma) - \cdots] - [-u_1 f_u^2\cos(f_u\tau \\ &\quad - \gamma)]\sin\alpha\tau[2J_1\cos(f_u\tau - \gamma) - 2J_3\cos 3(f_u\tau - \gamma) \\ &\quad + 2J_5\cos 5(f_u\tau - \gamma) - \cdots]\}\end{aligned} \tag{30}$$

where J's represent the Bessel's coefficients as the above. The equation can be expanded with trigonometric function, and the expanding harmonic terms with the lowest frequency are kept. Also, there are no harmonic functions with frequency 2α existed in the expansion. Thus, the nonlinear term $\varepsilon(\theta'')\cos\theta$ is equated with $\sin\alpha\tau$ and $\cos\alpha\tau$ as follows:

$$\begin{aligned}\varepsilon\theta''\cos\theta &= \varepsilon\sin(\alpha\tau)\left[(u_1 f_u^2)J_1 + (-u_1 f_u^2)\frac{J_0 - J_2}{2}\sin\gamma\right] \\ &\quad + \varepsilon\cos(\alpha\tau)\left[(-u_1 f_u^2)\frac{J_0 - J_2}{2}\cos\gamma\right]\end{aligned} \tag{31}$$

Substituting Eqs. (16) and (17) together with Eqs. (28) and (31) into Eq. (22) yields

$$\begin{aligned}&L(V_{1q}) - \varepsilon\sin(\alpha\tau)\left[\left(\alpha^2 + \frac{u_1^2 f_u^2}{2}\right)J_0 + \left(\alpha^2 + \frac{u_1^2 f_u^2}{2}\right)J_1\sin\gamma\right. \\ &\quad + (-2\alpha u_1 f_u)\frac{J_0 + J_2}{2}\sin\gamma - \left(-\frac{u_1^2 f_u^2}{2}\right)J_2 \\ &\quad \left. + \left(-\frac{u_1^2 f_u^2}{2}\right)\frac{J_1 - J_3}{2}\sin\gamma\right] - \varepsilon\cos(\alpha\tau)\left[\left(\alpha^2 + \frac{u_1^2 f_u^2}{2}\right)J_1\cos\gamma\right. \\ &\quad \left. + (-2\alpha u_1 f_u)\frac{J_0 + J_2}{2}\cos\gamma + \left(-\frac{u_1^2 f_u^2}{2}\right)\frac{J_1 - J_3}{2}\cos\gamma\right] \\ &\quad + \varepsilon\sin(\alpha\tau)\left[(u_1 f_u^2)J_1 + (-u_1 f_u^2)\frac{J_0 - J_2}{2}\sin\gamma\right] + \varepsilon\cos(\alpha\tau) \\ &\quad \times\left[(-u_1 f_u^2)\frac{J_0 - J_2}{2}\cos\gamma\right] - q_1\alpha^2\cos(\alpha\tau - \beta) \\ &\quad - 2\rho q_1\alpha\sin(\alpha\tau - \beta) + q_1\cos(\alpha\tau - \beta) - F_{\text{eq}}(\tau) = 0\end{aligned} \tag{32}$$

where $J_0 \approx 1$, $J_1 \approx u_1/2$, $J_2 \approx 0$, and $J_3 \approx 0$ if $|u_1| < 0.5$. Then, after equating the harmonic function with the same frequency, Eq. (32) becomes

$$\begin{aligned}&L(V_{1q}) + (-\varepsilon\alpha^2 - q_1\alpha^2\sin\beta - 2\rho q_1\alpha\cos\beta + q_1\sin\beta) \\ &\quad \times\sin\alpha\tau + (-\varepsilon\alpha^2 J_1\cos\gamma - q_1\alpha^2\cos\beta + 2\rho q_1\alpha\sin\beta \\ &\quad + q_1\cos\beta)\cos\alpha\tau - F_{\text{eq}}(\tau) = 0\end{aligned} \tag{33}$$

Meanwhile, because $|u_1| < 0.5$, the terms with u_1^2 of Eq. (33) can be ignored. After that, Eq. (33) can be solved using the variational method [17]:

$$V_{1q}(t)=\int_0^{\tau}\sin(t-\tau)\Bigg\{[(1-\alpha^2)q_1\sin\beta-2\rho q_1\alpha\cos\beta-\varepsilon\alpha^2]\sin\alpha t dt+\Bigg[(1-\alpha^2)q_1\cos\beta+2\rho q_1\alpha\sin\beta-\frac{1}{2}\varepsilon\alpha^2u_1\cos\gamma\Bigg]\cos\alpha t-F_{\mathrm{eq}a}(\tau)\Bigg\}dt=\frac{1}{1-\alpha^2}\Bigg\{[(1-\alpha^2)q_1\sin\beta-2\rho q_1\alpha\cos\beta-\varepsilon\alpha^2][-\sin(\alpha\tau)+\alpha\sin(\tau)]+\Bigg[(1-\alpha^2)q_1\cos\beta+2\rho q_1\alpha\sin\beta-\frac{1}{2}\varepsilon\alpha^2u_1\cos\gamma\Bigg]\times[-\cos(\alpha\tau)+\cos(\tau)]-\frac{F}{(M+m)Rw_n^2}[-\cos(\alpha\tau)+\cos(\tau)]\Bigg\} \tag{34}$$

In order to prevent the secular terms from occurring in the next iteration [14], we set the coefficients of $\cos\tau$ and $\sin\tau$ to zero to yield

$$(1-\alpha^2)q_1\sin\beta-2\rho q_1\alpha\cos\beta-\varepsilon\alpha^2=0 \tag{35}$$

$$(1-\alpha^2)q_1\cos\beta+2\rho q_1\alpha\sin\beta-\tfrac{1}{2}\varepsilon\alpha^2u_1\cos\gamma-F_{\mathrm{eq}}=0 \tag{36}$$

Herein, the first-order approximation is obtained,

$$V_q(\tau)=q_1\cos(\alpha\tau-\beta) \tag{37}$$

Similar to the above manipulation for obtaining the approximate solution for Eq. (7), with the initial approximation of Eq. (17), two equations can be obtained from Eq. (15) as follows:

$$L(V_{0\theta})-L(U_{0\theta})=0 \tag{38}$$

$$L(V_{1\theta})+N(V_{0\theta q})+L(U_{0\theta})=0 \tag{39}$$

From Eq. (38), we have

$$V_{0\theta}=U_{0\theta}=\alpha\tau+u_1\cos(2\alpha\tau-\gamma) \tag{40}$$

For Eq. (39), the nonlinear term includes $q''\cos\theta$ of Eq. (8), and others belong to linear terms. The nonlinear term can be written based on the above similar derivation as

$$q''\cos\theta=\sin(2\alpha\tau)\Big\{\tfrac{1}{2}(-q_1f_q^2)[-J_0\sin(-\beta)+J_2\sin(\beta-2\gamma)+J_1\cos(-\beta-\gamma)-J_1\cos(\beta-\gamma)]\Big\}+\cos(2\alpha\tau)\times\Big\{\tfrac{1}{2}(-q_1f_q^2)[J_0\cos(-\beta)-J_2\cos(\beta-2\gamma)+J_1\times\sin(-\beta-\gamma)-J_1\sin(\beta-\gamma)]\Big\}+\tfrac{1}{2}(-u_1f_u^2)[J_0\times\cos(-\beta)+J_1\sin(\beta-\gamma)] \tag{41}$$

with J's representing the Bessel's coefficients as Eq. (27). Substituting Eqs. (17) and (41) into Eq. (39) yields

$$L(V_{1\theta})+\sin(2\alpha\tau)\Big\{\tfrac{1}{2}(-q_1f_q^2)[-J_0\sin(-\beta)+J_2\sin(\beta-2\gamma)+J_1\cos(-\beta-\gamma)-J_1\cos(\beta-\gamma)]\Big\}+\cos(2\alpha\tau)\Big\{\tfrac{1}{2}(-q_1f_q^2)\times[J_0\cos(-\beta)-J_2\cos(\beta-2\gamma)+J_1\sin(-\beta-\gamma)-J_1\sin(\beta-\gamma)]\Big\}+\tfrac{1}{2}(-q_1f_q^2)[J_0\cos(-\beta)+J_1\sin(\beta-\gamma)]+(1+I_{\mathrm{eq}})\times(-u_1f_u^2)\cos\gamma\cos(2\alpha\tau)+(1+I_{\mathrm{eq}})(-u_1f_u^2)\sin\gamma\sin(2\alpha\tau)+\varsigma_m\alpha+\varsigma_m(-u_1f_u)\cos\gamma\sin(2\alpha\tau)-\varsigma_m(-u_1f_u)\sin\gamma\cos(2\alpha\tau)=0 \tag{42}$$

After equating the same trigonometric function, Eq. (42) becomes

$$L(V_{1\theta})+\Big[(1+I_{\mathrm{eq}})(-u_1f_u^2)\sin\gamma+\varsigma_m(-u_1f_u)\cos\gamma+\tfrac{1}{2}q_1\alpha^2\times\sin(-\beta)\Big]\sin(2\alpha\tau)+\Big[(1+I_{\mathrm{eq}})(-u_1f_u^2)\cos\gamma-\varsigma_m(-u_1f_u)\sin\gamma-\tfrac{1}{2}q_1\alpha^2\cos(-\beta)\Big]\cos(2\alpha\tau)+\tfrac{1}{2}(-q_1f_q^2)J_0\times\cos(-\beta)+\tfrac{1}{2}(-q_1f_q^2)J_1\sin(\beta-\gamma)+\varsigma_m\alpha=0 \tag{43}$$

where $J_0\approx1$ and $J_1\approx u_1/2$ from Eq. (25) with $|u_1|<0.5$. Similarly, because $|u_1|<0.5$, the terms with u_1^2 of Eq. (43) can be ignored. Then, with the expansion and simplification of equations, there is one equation left without the harmonic term of frequency 2α:

$$\tfrac{1}{2}(-q_1f_q^2)J_0\cos(-\beta)+\tfrac{1}{2}(-q_1f_q^2)J_1\sin(\beta-\gamma)+\varsigma_m\alpha=0 \tag{44}$$

Hence, the rest solution for Eq. (43) can be derived using the variational method [17]:

$$V_{1\theta}(t)=\int_0^{\tau}\sin(t-\tau)\Bigg\{\Bigg[(1+I_{\mathrm{eq}})(-u_1f_u^2)\sin\gamma+\varsigma_m(-u_1f_u)\cos\gamma+\frac{1}{2}q_1\alpha^2\sin(-\beta)\Bigg]\sin2\alpha t+\Bigg[(1+I_{\mathrm{eq}})(-u_1f_u^2)\cos\gamma-\varsigma_m(-u_1f_u)\sin\gamma-\frac{1}{2}q_1\alpha^2\cos(-\beta)\Bigg]\cos2\alpha t\Bigg\}dt=\frac{1}{1-4\alpha^2}\Bigg\{\Bigg[(1+I_{\mathrm{eq}})(-4\alpha^2u_1)\sin\gamma-2\varsigma_mu_1\alpha\cos\gamma+\frac{1}{2}q_1\alpha^2\sin(-\beta)\Bigg][2\alpha\sin\tau-\sin2\alpha\tau]\Bigg[(1+I_{\mathrm{eq}})\times(-4\alpha^2u_1)\cos\gamma+2\varsigma_mu_1\alpha\sin\gamma-\frac{1}{2}q_1\alpha^2\cos(-\beta)\Bigg]\times[-\cos2\alpha\tau+\cos\tau]\Bigg\} \tag{45}$$

To prevent the secular terms that may occur in the next iteration [14], the coefficients of $\cos\tau$ and $\sin\tau$ are set to zero to yield

$$(1+I_{\mathrm{eq}})(-4\alpha^2u_1)\sin\gamma-2\varsigma_mu_1\alpha\cos\gamma+\tfrac{1}{2}q_1\alpha^2\sin(-\beta)=0 \tag{46}$$

$$(1+I_{\mathrm{eq}})(-4\alpha^2u_1)\cos\gamma+2\varsigma_mu_1\alpha\sin\gamma-\tfrac{1}{2}q_1\alpha^2\cos(-\beta)=0 \tag{47}$$

Thus, the first-order approximation is obtained

$$V_{\theta}(\tau)=\alpha\tau+u_1\cos(2\alpha\tau-\gamma) \tag{48}$$

On the basis of the four Eqs. (35), (36), (46), and (47), the four unknowns q_1, u_1, β, and γ can be solved as

$$q_1=Tu_1 \tag{49}$$

$$u_1=\frac{\varepsilon\alpha^2}{(1-\alpha^2)T\sin\beta-2\rho\alpha T\cos\beta} \tag{50}$$

$$\beta=\tan^{-1}\Bigg\{\frac{\varepsilon\alpha^2\Big[(1-\alpha^2)T-\frac{1}{2}\varepsilon\alpha^2\cos\phi\Big]+2F_{\mathrm{eq}}\rho\alpha T}{\varepsilon\alpha^2\Big[-2\rho\alpha T+\frac{1}{2}\varepsilon\alpha^2\sin\phi\Big]+F_{\mathrm{eq}}(1-\alpha^2)T}\Bigg\} \tag{51}$$

$$\gamma=\beta-\phi \tag{52}$$

where

$$T = -4\sqrt{4(1+I_{eq})^2 + \frac{s_m^2}{\alpha^2}}$$

$$\phi = \tan^{-1}\left(\frac{s_m}{2\alpha(1+I_{eq})}\right)$$

4 Stability Analysis

Having derived the first-order approximate steady-state solutions of the reciprocating main mass and the rotational free mass, the solutions are accompanied with the Newton method for acquiring the accurate values. Subsequently, the stability analysis is initiated by providing small perturbations $\tilde{q}$ and $\tilde{\theta}$ to the solutions, yielding

$$q = q_1 \cos(f_q \tau - \beta) + \tilde{q} \tag{53}$$

$$\theta = \alpha\tau + u_1 \cos(f_u \tau - \gamma) + \tilde{\theta} \tag{54}$$

Substituting the perturbed q and θ of Eqs. (53) and (54) into Eqs. (7) and (8) yields the equations with the linear parts in terms of the perturbations $\tilde{q}$ and $\tilde{\theta}$ as

$$\tilde{q}'' + 2\rho\tilde{q}' + \tilde{q} + p_1\tilde{\theta}'' + p_2\tilde{\theta}' + p_3\tilde{\theta} = 0 \tag{55}$$

$$\tilde{\theta}'' + \frac{s_m}{1+I_{eq}}\tilde{\theta}' + p_4\tilde{\theta} + p_5\tilde{q}'' = 0 \tag{56}$$

where the expressions of p_s' are used for presentation simplicity. They are

$$p_1 = \varepsilon \cos\theta_b \tag{57}$$

$$p_2 = -2\varepsilon[(-u_1 f_u)\sin\psi + \alpha]\sin\theta_b \tag{58}$$

$$p_3 = -\varepsilon\{[\alpha^2 + (-u_1 f_u)^2 \sin^2\psi + 2\alpha(-u_1 f_u)\sin\psi]\cos\theta_b + (-u_1 f_u^2)\cos\psi\sin\theta_b\} \tag{59}$$

$$p_4 = \frac{(q_1 f_q^2)\cos\eta\sin\theta_b}{1+I_{eq}} \tag{60}$$

$$p_5 = \frac{\cos\theta_b}{1+I_{eq}} \tag{61}$$

with

$$\theta_b = \alpha\tau + u_1\cos\psi$$

$$\psi = f_u\tau - \gamma$$

$$\eta = f_q\tau - \beta$$

Equations (55) and (56) are, in fact, linearized state equations with periodic coefficients. The well-known Floquet theory [18] is, therefore, employed to investigate the stabilities of the solved approximate steady-state solutions [19]. By assuming $\tilde{q}' = \tilde{Q}$ and $\tilde{\theta}' = \tilde{O}$, the two second-order Eqs. (55) and (56) could be transformed into four first-order equations as

$$\tilde{x}' = A(\tau)\tilde{x} \tag{62}$$

where $A(\tau)$ is the so-called transition matrix, which is computed over one period. On the basis of the magnitudes of eigenvalues of the transition matrix, the stability of each solved steady-state solution is determined. If the magnitudes of eigenvalues of the transition matrix are >1, then the solved solutions are unstable and cannot be observed at the steady state. However, if the magnitudes of eigenvalues of the transition matrix are <1, then the solved solutions are stable and the hula-hoop motion will appear.

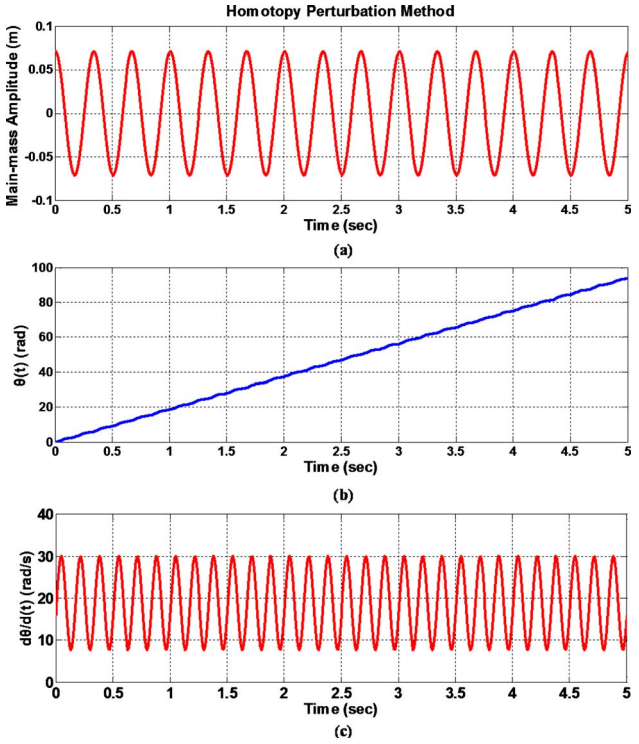

Fig. 2 (*a*) Amplitude of the main mass, (*b*) angular displacement, and (*c*) angular velocity of the free mass. All were solved by the homotopy perturbation method.

5 Results and Discussion

When the main mass vibrates harmonically, the ideal hula-hoop motion is defined as follows: The free mass is continuously spinning around the center of the main mass in one direction without oscillation. Here, we first examine the accuracy of the physical model by observing the dynamic response of the main mass as well as the free mass based on the approximate solutions obtained by applying the homotopy perturbation method, i.e., Eqs. (37) and (48), and the direct numerical simulation of Eqs. (5) and (6). Second, stability analysis is performed to confirm the existence of the hula-hoop motion. To emphasize the effect of the mass moment of inertia of the free mass on the existence of hula-hoop motion, Figs. 2–5 are plotted based on the results without the mass moment of inertia of the free mass.

5.1 Dynamic Responses of the Main and Free Masses. The system parameters and initial conditions (ICs) employed in the simulation are listed in Table 1. Taking the frequency of 3 Hz and amplitude of 60 N of the excitation force as an example, the results are first obtained on the basis of the approximate solutions and are shown in Fig. 2. Figure 2(*a*) shows the main mass reciprocating harmonically with a stable frequency, ω, which is relevant to the excitation force. Figure 2(*b*) demonstrates that the free mass spins continuously in the same direction; this figure also illustrates that the slope of the angular variation is related to the excitation frequency ω but with small oscillations, which indicates that the free mass has nonconstant angular velocity, as shown in Fig. 2(*c*). The similar results shown in Figs. 3(*a*)–3(*c*) are attained by numerical simulation with MATLAB. Except within the transient state from 0 s to 1.5 s, the hula-hoop motion follows immediately. From the figures, it can be seen that the main mass reciprocates harmonically and the free mass is in continuous rotation but is accompanied with small oscillation in a frequency doubling the oscillating frequency of the main mass.

To this end, Figs. 2 and 3 confirm the accuracy of the physical model of hula-hoop motion, the governing equations, and solution

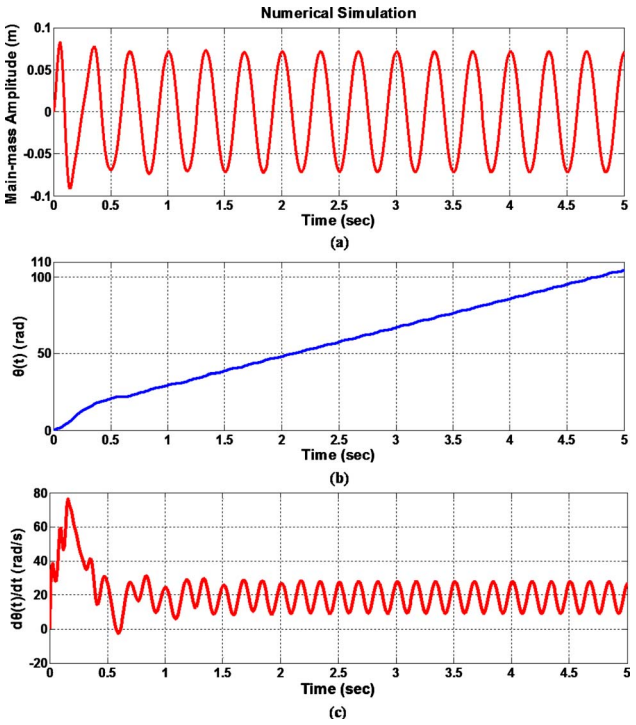

Fig. 3 (*a*) Amplitude of the main mass, (*b*) angular variation, and (*c*) angular velocity of the free mass. All were solved by direct numerical simulation.

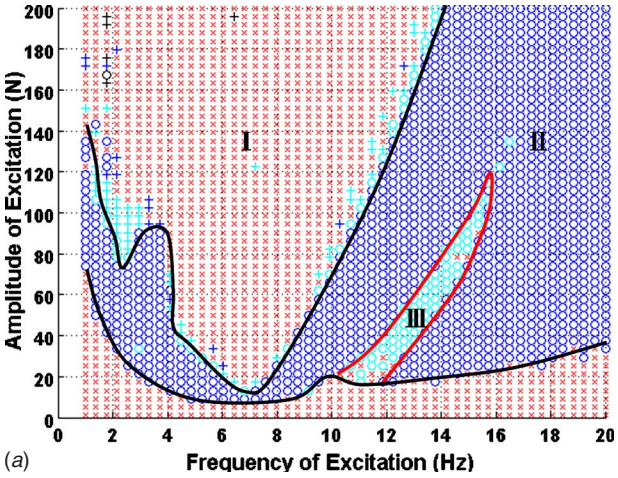

(*a*)

	Blue (o)	Blue (+)	Cyan (o)	Cyan (+)	Red (×)
Hula-hoop motion	Yes	No	No	No	No
Reversal	No	Yes	No	Yes	Yes
Freq. α	$\fallingdotseq 1\omega$	$\fallingdotseq 1\omega$	$\fallingdotseq 1\omega$	$\fallingdotseq 1\omega$	$=0\omega$
Freq. *fu*	$\fallingdotseq 2\omega$	$\fallingdotseq 2\omega$	$\neq 2\omega$	$\neq 2\omega$	

(*b*)

Fig. 5 Occurrence of hula-hoop motion obtained from direct numerical simulation

methods. Although the angular velocity of the free mass oscillates at the transient state, it still possesses continuous rotation at the steady state.

5.2 Approximate and Numerical Integrated Results. Figure 4 shows the stability of the approximate solutions obtained by using the homotopy perturbation method. The zone with blue o's in region II is stable; it is where the hula-hoop motion exists.

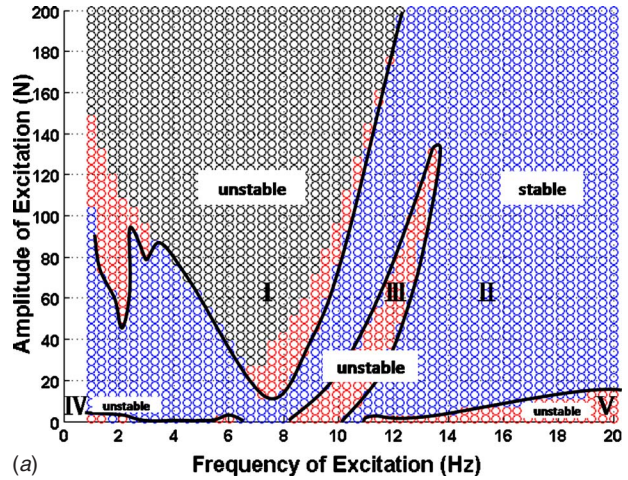

(*a*)

	Blue (○)	Red (○)	Black (○)
$\lvert u_1\rvert$	$\lvert u_1\rvert<0.5$	$\lvert u_1\rvert<0.5$	$\lvert u_1\rvert\geqq 0.5$
Hula-hoop motion	Yes	No	No

(*b*)

Fig. 4 Stability of the approximate solutions

Within this zone, the main mass reciprocates in the y-direction with frequency ω and the free mass rotates continuously at the speed ω, which is accompanied by angular oscillation at a frequency of 2ω. The zones with red and black o's in region I and the zones with red o's in regions III, IV, and V are unstable, indicating that steady-state hula-hoop motion does not exist. Furthermore, the unstable zones with red and black o's feature $|u_1|<0.5$ and $|u_1|\geq 0.5$, respectively. Hence, it is essential to maintain the value of $|u_1|<0.5$ under certain combinations of frequencies and amplitudes of excitations to ensure the existence of hula-hoop motion.

At the red zone, even with $|u_1|<0.5$, the system has no hula-hoop motion because the free mass moves alternatively; that is, the free mass possesses reversal motion. In the same zone, as $|u_1|$ increases, the free mass is accompanied with larger reversal motion. Thus, it is necessary to observe the effect of $|u_1|$ on the motion of free mass. It appears that the system featuring larger $|u_1|$ causes larger reversal motion.

Figure 5 shows the results obtained from direct numerical integration, which can be used to confirm the effectiveness of the stability analysis, as shown in Fig. 4, which is conducted by using

Table 1 System parameters and ICs

Properties	Symbol	Value (Unit)
Main mass	M	0.45 kg
Free mass	m	0.045 kg
Mass ratio $(m/(M+m))$	ε	0.09
Rotational radius of free mass	R_m	0.05 m
Damping ratio	C	0.1
Coefficient of spring	K	1000 N/m
Damping ratio of free mass	c_m	0.01
IC of main mass	$y(0)$	0 m
IC of main mass	$y'(0)$	0 m/s
IC of free mass	$\theta(0)$	0.0 rad
IC of free mass	$\theta'(0)$	0.0 rad/s

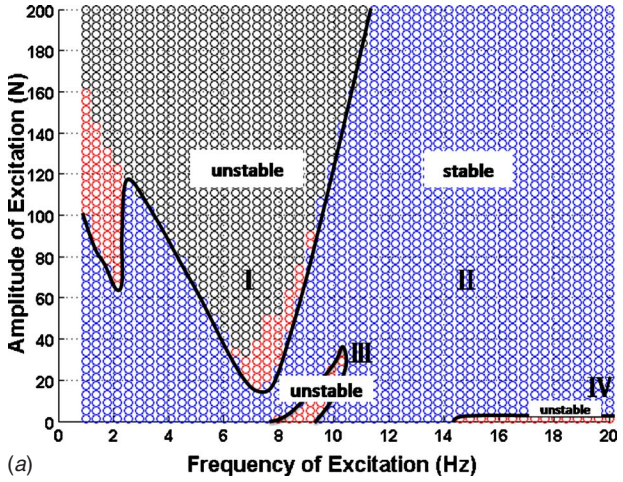

(*a*)

(*b*)

	Blue (○)	Red (○)	Black (○)
$\lvert u_1 \rvert$	$\lvert u_1 \rvert < 0.5$	$\lvert u_1 \rvert < 0.5$	$\lvert u_1 \rvert \geqq 0.5$
Hula-hoop motion	Yes	No	No

Fig. 6 Stability of the approximate solutions with the moment of inertia of free mass

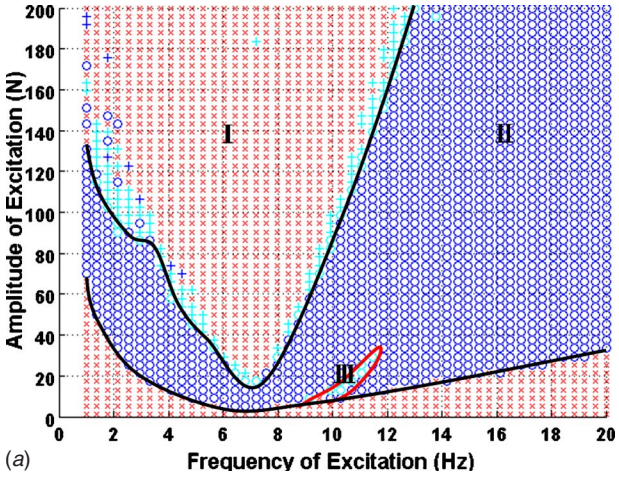

(*a*)

(*b*)

	Blue (o)	Blue (+)	Cyan (o)	Cyan (+)	Red (×)
Hula-hoop motion	Yes	No	No	No	No
Reversal	No	Yes	No	Yes	Yes
Freq. α	$\fallingdotseq 1\omega$	$\fallingdotseq 1\omega$	$\fallingdotseq 1\omega$	$\fallingdotseq 1\omega$	$= 0\omega$
Freq. fu	$\fallingdotseq 2\omega$	$\fallingdotseq 2\omega$	$\neq 2\omega$	$\neq 2\omega$	

Fig. 7 Occurrence of hula-hoop motion obtained from direct numerical simulation with the moment of inertia of free mass

the approximate solutions and the Floquet theory [18]. Good agreement between these two figures implies the feasibility of the homotopy perturbation method. Figure 5 shows that the dynamic system of region II, represented by blue o's, is stable and the hula-hoop motion occurs. However, the system of region I that is represented by red ×'s is unstable, which means that there is no hula-hoop motion but with reversal motions instead. In addition, there are certain transition regions represented by cyan +'s between regions I and II where the free mass of the system has no hula-hoop motion but exhibits repeated reversals. Note that the system in region III that is represented by the cyan o's demonstrates hula-hoop motion at the transient state and oscillates with a different frequency. However, it becomes unstable at a steady-state condition, i.e., no hula-hoop motion.

In Figs. 4 and 5, it can be seen that the stability analysis performed using the approximate solutions from the homotopy perturbation method may be less accurate than that of direct numerical integration. The reason is that only the α oscillation term in Eq. (7) and the 2α term in Eq. (8) are evaluated. Thus, the effect of high frequency oscillation terms is omitted in the stability analysis for simplicity. Moreover, the oscillation term of the free mass $u_1 \cos(f_u \tau - \gamma)$ may cause reversals if $|u_1| \geq 0.5$ when the free mass revolves. Hence, the design engineer should keep u_1 as small as possible to ensure that the free mass rotates smoothly with small vibrations.

Figure 6 presents the stability of hula-hoop motion attained by using the homotopy perturbation method as the mass moment of inertia of free mass is taken into consideration. It shows three unstable regions, I, III, and IV, with decreased areas in comparison with those of Fig. 4. The left section of the unstable zone I is decreased when compared with Fig. 4, where there exists a downward zone extending into the stable region. Under the same conditions, the slim unstable zone III also decreases. Figure 7 shows the results with consideration of the moment of inertia of free mass by using direct numerical integration. Good agreement between Figs. 6 and 7 is also achieved. In Fig. 7, it can be seen that the unstable region III diminishes compared with that of Fig. 5, and the left part of region I also reduces. The zone with cyan "o" in region I, compared with that of Fig. 5, decreases, and it has hula-hoop motion at the transient state but not at the final steady state. Therefore, from the result, it is determined that the hula-hoop motion is obtained more easily when the free mass has the mass moment of inertia.

6 Conclusion

This paper presents a thorough dynamic analysis for the proposed motion transformer mimicking a hula hoop. The physical model of the system was first constructed, and the governing equations were then derived by using Lagrange's method. By employing the homotopy perturbation method, the approximate solutions were attained, which was followed by stability analysis using the Floquet theory. The dynamic response and stability diagram were simultaneously acquired from direct numerical simulation using MATLAB. Good agreement between the results obtained from these two methods implies that the approximate solutions are adequate for the dynamic analysis of the proposed model. Furthermore, via the analysis based on the Floquet theory, the stability of the desired solution remains over a large set of combinations of excitation frequencies and amplitudes. Finally, the proposed motion transformer can be applied to energy scavenging systems, and the results may provide design guidelines for this class of systems.

Acknowledgment

The authors appreciate the support from the National Science Council of Taiwan under the Grant No. NSC 97-2221-E-007-050.

Appendix

Table 1 lists the system parameters and ICs.

References

[1] Yoshitake, Y., Ishibashi, T., and Fukushima, A., 2004, "Vibration Control and Electricity Generating Device Using a Number of Hula-Hoops and Generators," J. Sound Vib., **275**(1–2), pp. 77–88.
[2] Hatwal, H., Mallik, A. K., and Ghosh, A., 1983, "Forced Nonlinear Oscilla-

tions of an Autoparametric System—Part 1: Periodic Responses," ASME J. Appl. Mech., **50**, pp. 657–662.
[3] Garira, W., and Bishop, S. R., 2003, "Rotating Solutions of the Parametrically Excited Pendulum," J. Sound Vib., **263**(1), pp. 233–239.
[4] Lenci, S., Pavlovskaia, E., Rega, G., and Wiercigroch, M., 2008, "Rotating Solutions and Stability of Parametric Pendulum by Perturbation Method," J. Sound Vib., **310**(1–2), pp. 243–259.
[5] Wu, S. T., 2009, "Active Pendulum Vibration Absorbers With a Spinning Support," J. Sound Vib., **323**(1–2), pp. 1–16.
[6] Nayfeh, A. H., and Mook, D. T., 1979, *Nonlinear Oscillations*, Wiley, New York.
[7] Broek, B. V. D., and Verhulst, F., 1987, "Averaging Techniques and the Oscillator-Flywheel Problem," Nieuw Arch. Wiskd., **5**(2), pp. 185–206.
[8] Rand, R. H., Kinsey, R. J., and Mingori, D. L., 1992, "Dynamics of Spinup Through Resonance," Int. J. Non-Linear Mech., **27**(3), pp. 489–502.
[9] Quinn, D., and Rand, R., 1995, "The Dynamics of Resonant Capture," Nonlinear Dyn., **8**(1), pp. 1–20.
[10] Quinn, D. D., 1997, "Resonance Capture in a Three Degree-of-Freedom Mechanical System," Nonlinear Dyn., **14**(4), pp. 309–333.
[11] Balthazar, J. M., Cheshankov, B. I., Ruschev, D. T., Barbanti, L., and Weber, H. I., 2001, "Remarks on the Passage Through Resonance of a Vibrating System With Two Degrees of Freedom, Excited by a Non-Ideal Energy Source," J. Sound Vib., **239**(5), pp. 1075–1085.
[12] Bolla, M. R., Balthazar, J. M., Felix, J. L. P., and Mook, D. T., 2007, "On an Approximate Analytical Solution to a Nonlinear Vibrating Problem, Excited by a Nonideal Motor," Nonlinear Dyn., **50**(4), pp. 841–847.
[13] Batiha, B., Noorani, M. S. M., and Hashim, I., 2008, "Numerical Solutions of the Nonlinear Integro-Differential Equations," Int. J. Open Problems Compt. Math., **1**(1), pp. 34–42.
[14] He, J. H., 2000, "A Coupling Method of a Homotopy Technique and a Perturbation Technique for Nonlinear Problems," Int. J. Non-Linear Mech., **35**, pp. 35–43.
[15] He, J. H., 2003, "Homotopy Perturbation Method: A New Nonlinear Analytical Technique," Appl. Math. Comput., **135**, pp. 73–79.
[16] Whittaker, E. T., and Watson, G. N., 1958, *A Course of Modern Analysis*, Cambridge University Press, Cambridge, UK.
[17] He, J. H., 1999, "Variational Iteration Method—A Kind of Nonlinear Analytical Technique: Some Examples," Int. J. Non-Linear Mech., **34**, pp. 699–708.
[18] Kapitaniak, T., and Bishop, S. R., 1999, *The Illustrated Dictionary of Nonlinear Dynamics and Chaos*, Wiley, Chicester, UK.
[19] Meirovitch, L., 2001, *Fundamentals of Vibrations*, McGraw-Hill, Singapore.